Hydrogen Production

DOI: 10.1002/ange.200803899

Simultaneous Production of Hydrogen and Synthesis Gas by Combining Water Splitting with Partial Oxidation of Methane in a Hollow-Fiber Membrane Reactor**

Heqing Jiang, Haihui Wang, Steffen Werth, Thomas Schiestel, and Jürgen Caro*

Hydrogen is gaining more and more attention because it is regarded as an important future fuel. Today, hydrogen is mainly produced from nonrenewable natural gas and petroleum. With concerns over worldwide energy demands and global climate change, alternative sources must be found. Obviously, water is recommended as the ideal source for the generation of large amounts of hydrogen.[1] In addition to electrolysis, recently several new processes, such as photovoltaic–photoelectrochemical water splitting[2–4] and one-step or multistep thermochemical water splitting[5,6] based on focused solar[7–9] or nuclear[10] heat, have been developed. Although water dissociation into oxygen and hydrogen is conceptually simple [Eq. (1)], efficient hydrogen production

$$H_2O \rightleftharpoons H_2 + {}^1/_2O_2 \qquad (1)$$

from water remains difficult as a result of the low equilibrium constant of $K_p \approx 2 \times 10^{-8}$ at the relatively high temperature of 950 °C.[11]

However, the hydrogen production rate can be significantly improved by extracting oxygen with an oxygen-permeable membrane. One possible type of membrane for the efficient removal of oxygen at high temperatures is a mixed oxygen-ion- and electron-conducting membrane (MIECM) with high oxygen permeability.[12–16] Early studies demonstrated the possibility of hydrogen production through direct water decomposition by using MIECMs at the extremely high temperature of 1400–1800 °C.[17–20] However, the hydrogen production rate was relatively low because of the poor oxygen permeability of these membranes, and only a modest rate of 0.6 $cm^3 min^{-1} cm^{-2}$ could be obtained at 1683 °C.[19] To obtain a higher hydrogen production rate, one possible way is to increase the rate of oxygen removal. Balachandran et al. fed hydrogen on the permeation side of a MIECM to consume the permeated oxygen.[21,22] In this case, a high oxygen partial pressure gradient across the membrane was established and a maximum hydrogen production rate of 10.0 $cm^3 min^{-1} cm^{-2}$ at 900 °C was obtained.[21,22] However, the amount of hydrogen produced was equivalent to the amount consumed, which makes it unpractical. Therefore, it would be attractive for both the feed and permeate stream to yield a valuable compound.

Herein, for the first time we report the simultaneous production of hydrogen and synthesis gas in a hollow-fiber perovskite MIECM reactor using methane to consume the permeated oxygen (see Figure 1). At high temperatures, water dissociates into hydrogen and oxygen on the membrane surface of the core side. Oxygen permeates from the core to the shell side of the hollow fiber, where it is consumed by the partial oxidation of methane (POM) to form synthesis gas according to $CH_4 + {}^1/_2O_2 \rightarrow CO + 2H_2$. Thus, when operating under equilibrium-controlled conditions, the water dissociation proceeds continuously as the oxygen is continuously consumed by the POM to produce synthesis gas. The advantage of this process is to give pure hydrogen as well as synthesis gas, which can be used to synthesize a wide variety of valuable hydrocarbons (for example, by Fischer–Tropsch synthesis) and oxygenates (methanol).

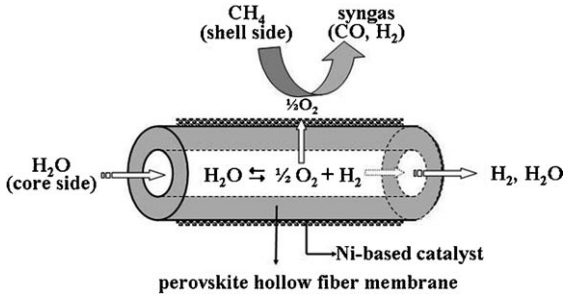

Figure 1. The concept of simultaneous production of hydrogen and synthesis gas by combining water splitting with POM in a perovskite oxygen-permeable hollow-fiber membrane.

A novel $BaCo_xFe_yZr_{1-x-y}O_{3-\delta}$ (BCFZ) perovskite hollow-fiber membrane was applied for the in situ removal of the oxygen that is produced by high-temperature water splitting,

[*] Prof. Dr. H. Wang
School of Chemistry & Chemical Engineering
South China University of Technology
Wushan Road, Guangzhou 510640 (P.R. China)
Fax: (+86) 20-87110131
E-mail: hhwang@scut.edu.cn
H. Jiang, Prof. Dr. J. Caro
Institute of Physical Chemistry and Electrochemistry, Leibniz University of Hanover (Germany)
Dr. S. Werth
Uhde GmbH, Dortmund (Germany)
Dr. T. Schiestel
Fraunhofer Institute of Interfacial Engineering and Biotechnology (IGB), Stuttgart (Germany)

[**] We gratefully acknowledge the financial support of the BMBF for project 03C0343A under the auspices of ConNeCat and H.W. thanks the NSFC (No.2070620) for financial support.

Supporting information for this article is available on the WWW under http://dx.doi.org/10.1002/anie.200803899.

because it exhibits a high oxygen permeation rate[23–25] and has already been used, for example, in the production of oxygen-enriched air[26,27] and the partial oxidation of hydrocarbons.[28,29] Figure 2 shows the influence of temperature on

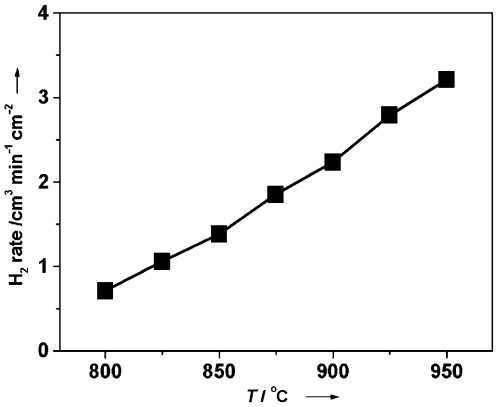

Figure 2. H_2 production rate on the core side as a function of temperature. Core side: flow rate $F_{H_2O} = 30$ and $F_{He} = 10\ cm^3\,min^{-1}$; shell side: $50\ cm^3\,min^{-1}$ ($F_{He} = 45$, $F_{Ne} = 3$, and $F_{CH_4} = 2\ cm^3\,min^{-1}$). Amount of packed Ni/Al_2O_3 catalyst: 0.8 g. Effective membrane area: 0.86 cm^2.

the hydrogen production rate. This rate increases as the temperature rises from 800 to 950 °C and a hydrogen flux of $3.1\ cm^3\,min^{-1}\,cm^{-2}$ was obtained at 950 °C. It was also found that the hydrogen production rate is very low ($< 0.026\ cm^3\,min^{-1}\,cm^{-2}$ at 900 °C, see Figure S1 in the Supporting Information) if a sweep gas, such as He, is used on the permeate side.

Clearly, the hydrogen production rate depends directly on the rate of oxygen removal from the water dissociation system. The oxygen transport can be described by the Wagner equation for the oxygen flux $j(O_2)$ [Eq. (2)],[30,31] where σ_{el} and

$$j(O_2) = -\frac{1}{(4F)^2}\frac{\sigma_{el}\,\sigma_{ion}}{\sigma_{el}+\sigma_{ion}}\nabla\mu_{O_2} \text{ with } \nabla\mu_{O_2} = \frac{\partial R\,T\ln a_{O_2}}{\partial x} \qquad (2)$$

σ_{ion} are the electronic and ionic conductivities, respectively, F the Faraday constant, and $\bigtriangledown\mu_{O_2}$ the gradient of the chemical potential of oxygen across the membrane. Assuming that $\sigma_{el} \gg \sigma_{ion}$ and that $\partial \ln a_{O_2}/\partial x$ can be approximated by $\ln(p'_{O_2}/p''_{O_2})/L$ with p'_{O_2} and p''_{O_2} denoting the oxygen partial pressures on the shell and core sides and L the membrane thickness, the Wagner equation reads [Eq. (3)]:

$$j(O_2) = -\frac{R\,T}{(4F)^2}\sigma_{ion}\frac{\ln(p'_{O_2}/p''_{O_2})}{L} \qquad (3)$$

The oxygen partial pressure p'_{O_2} on the permeate side can be reduced much more efficiently when feeding methane in combination with a Ni-based catalyst (Süd Chemie AG) to the shell side. The permeated oxygen on the shell side is then consumed very quickly by the oxidation of methane. As a result of the increased oxygen partial pressure gradient across the membrane, a higher hydrogen production rate of about $2.3\ cm^3\,min^{-1}\,cm^{-2}$ at 900 °C is obtained, which is two orders of magnitude higher than the rate of a nonreactive sweep gas such as He.

From the above discussion it follows that the hydrogen production rate is related to three reactions: water splitting, oxygen transport through the membrane, and POM. When the temperature is increased, the equilibrium constant of the endothermic water splitting will increase according to the Van't Hoff equation. So the equilibrium is shifted towards water dissociation and more hydrogen can be produced. Moreover, with increasing temperature, both the rate of the POM and the permeability of the BCFZ hollow-fiber membrane will increase. Thus, the hydrogen production rate becomes higher with increasing temperature.

With increasing concentration of steam in the feed gas on the core side, the equilibrium partial pressures of oxygen and hydrogen will increase, thus providing a higher driving force for oxygen permeation. As a result, the amount of hydrogen obtained is expected to increase. As shown in Figure 3, the

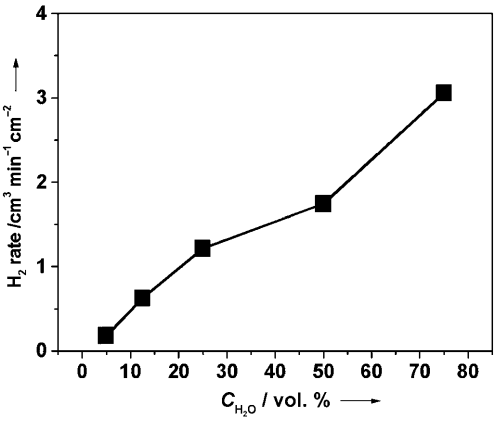

Figure 3. H_2 production rate on the core side at different steam concentrations. Core side (steam + He): $40\ cm^3\,min^{-1}$; shell side: $50\ cm^3\,min^{-1}$ ($F_{He} = 45$, $F_{Ne} = 3$, and $F_{CH_4} = 2\ cm^3\,min^{-1}$). Amount of packed Ni/Al_2O_3 catalyst: 0.8 g. Effective membrane area: 0.86 cm^2. $T = 950$ °C.

hydrogen production rate increased from about 0.2 to $3.1\ cm^3\,min^{-1}\,cm^{-2}$ when the steam concentration was changed from 5 to 75 vol.%. In addition, the hydrogen production rate can be enhanced by increasing the methane concentration (Figure 4), because a higher oxygen partial pressure gradient across the perovskite membrane is established, which leads to a higher oxygen permeation rate.

At the same time as hydrogen is produced on the core side of the BCFZ hollow fiber by water dissociation, synthesis gas can be produced on the shell side. Figure 5 shows the methane conversion and the CO selectivity for feeding different methane concentrations. When the amount of the feed gas methane was small, most of the methane was totally oxidized to give CO_2 and H_2O. On feeding more methane, the methane conversion decreased gradually and the CO selectivity increased. When $2\ cm^3\,min^{-1}$ methane diluted by $48\ cm^3\,min^{-1}$ inert gases was fed to the shell side, about 70% methane conversion and 60% CO selectivity were obtained. However, for high methane concentrations the calculated selectivities became lower again. This is probably

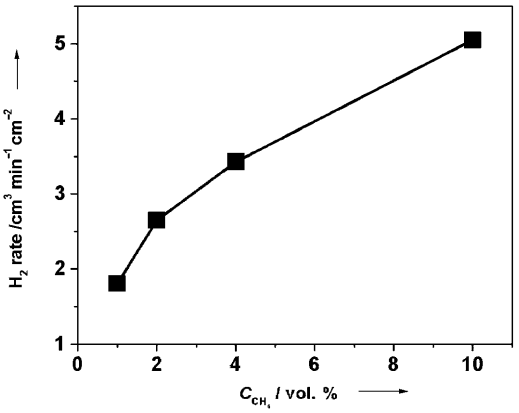

Figure 4. H_2 production rate on the core side at different methane concentrations. Core side: $F_{H_2O}=30$ and $F_{He}=10\ cm^3\,min^{-1}$; shell side: $50\ cm^3\,min^{-1}$ ($F_{Ne}=3$ and $F_{CH_4}+F_{He}=47\ cm^3\,min^{-1}$). Amount of packed Ni/Al_2O_3 catalyst: 0.8 g. Effective membrane area: 0.86 cm^2. $T=950\,°C$.

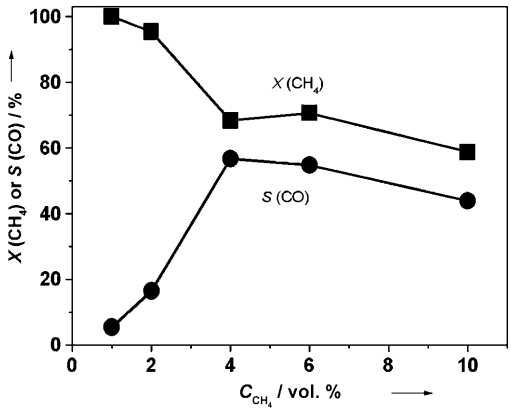

Figure 5. Conversion X of methane and selectivity S of CO on the shell side at different methane concentrations. Core side: $F_{H_2O}=30$ and $F_{He}=10\ cm^3\,min^{-1}$; shell side: $50\ cm^3\,min^{-1}$ ($F_{Ne}=3$ and $F_{CH_4}+F_{He}=47\ cm^3\,min^{-1}$). Amount of packed Ni/Al_2O_3 catalyst: 0.8 g. Effective membrane area: 0.86 cm^2. $T=950\,°C$.

caused by the formation of coke, which is expected to occur under these reaction conditions.

The net reaction in our concept is conventional methane steam reforming according to $H_2O+CH_4\rightarrow 3H_2+CO$ with a H_2/CO ratio of 3, which is unsuitable for the methanol or Fischer–Tropsch syntheses. However, in our process we obtain pure hydrogen on the core side as well as synthesis gas with a H_2/CO ratio of around 2 on the shell side. Synthesis gas with such a ratio is usually produced by oxygen-blown autothermal reforming, which requires a costly oxygen separation plant. Therefore, our concept provides a new way to obtain a Fischer–Tropsch synthesis gas. Furthermore, the pure hydrogen produced by our method can be used to operate the hydrocracking step in the product refinery section of the Fischer–Tropsch plant.

Hydrogen can also be produced with a hydrogen-selective membrane reactor in which methane steam reforming takes place with a reforming catalyst. The technology of steam reforming with hydrogen-selective Pd membranes has been developed since 1992 by Mitsubishi Heavy Industries and Tokyo Gas. The membrane reactor operates at 550 °C and produces 40 m^3 (STP) hydrogen h^{-1}.[32] However, the Pd/Pd alloy membrane can be poisoned by CO; therefore, a subsequent water-gas shift stage is needed to convert CO to CO_2, which makes the operation more complex. On the other hand, in the hydrogen-selective membrane reactor, only H_2 rather than synthesis gas can be obtained. In our concept, we can get both pure hydrogen, with an industrially interesting flux (ca. 3 $m^3\,h^{-1}\,m^{-2}$) without further water-gas shift reaction, and synthesis gas. Compared to conventional steam reforming and hydrogen-selective membrane-reactor-based steam reforming, our multifunctional reactor contributes to the concept of process intensification.

In conclusion, it is possible to produce significant amounts of hydrogen from water splitting at around 900 °C by using a novel BCFZ oxygen-permeable hollow-fiber membrane. By combining high-temperature water splitting with POM, not only hydrogen but also synthesis gas can be obtained. This process presents new insight into the interplay of catalysis and separation in a membrane reactor. Besides, abundant raw materials, such as water and methane (natural gas), were used, which is of broad interest.

Experimental Section

The dense BCFZ perovskite hollow-fiber membranes were manufactured by phase-inversion spinning followed by sintering.[23–29] The sintered fiber had a wall thickness of around 0.17 mm with an outer diameter of 1.10 mm and an inner diameter of 0.76 mm. Figure S2 in the Supporting Information shows a schematic diagram of the membrane reactor used in this study. Two ends of the hollow fiber were coated with Au paste. After sintering at 950 °C, a dense Au film that was not permeable to oxygen was obtained. Such an Au-coated hollow fiber was sealed by a silicon rubber ring and the uncoated part (3.0 cm), which was permeable to oxygen, was kept in the middle of the oven thus ensuring isothermal conditions. A mixture of steam and He was fed to the core side and a mixture of CH_4, Ne, and He was fed to the shell side. A Ni-based catalyst (Süd Chemie AG) was packed around and behind the hollow-fiber membrane. The CH_4, He, and Ne flow rates were controlled by gas mass-flow controllers (Bronkhorst). The H_2O flow was controlled by a liquid mass-flow controller (Bronkhorst) and completely evaporated at 180 °C before it was fed to the reactor. All gas lines to the reactor and the gas chromatograph were heated to 180 °C. The concentrations of the gases at the exit of the reactor were determined by an online gas chromatograph (Agilent 6890). Assuming that the oxygen from water splitting on the core side was totally removed and the flow rate at the outlet was equal to that at the inlet, the H_2 production rate after steam condensation in the retentate on the core side was calculated from the total flow rate F_{core} ($cm^3\,min^{-1}$), the hydrogen concentration $c(H_2)$, and the effective membrane area S (cm^2) based on Equation (4).

$$J(H_2)=\frac{F_{core}\,c(H_2)}{S} \tag{4}$$

The CH_4 conversion $X(CH_4)$ and the CO selectivity $S(CO)$ on the shell side were calculated as Equations (5) and (6), where $F(i)$ is the

$$X(CH_4)=\left(1-\frac{F(CH_4,out)}{F(CH_4,in)}\right)\times 100\,\% \tag{5}$$

$$S(\mathrm{CO}) = \frac{F(\mathrm{CO,out})}{F(\mathrm{CH_4,in}) - F(\mathrm{CH_4,out})} \times 100\,\% \qquad (6)$$

flow rate of species i on the shell side, calculated based on the measured concentration of the respective species and the total flow rate measured by a bubble flowmeter.

Received: August 7, 2008
Published online: October 23, 2008

Keywords: heterogeneous catalysis · hydrogen · perovskite · synthesis gas · water chemistry

[1] J. A. Turner, *Science* **2004**, *305*, 972 – 974.
[2] O. Khaselev, J. A. Turner, *Science* **1998**, *280*, 425 – 427.
[3] C. Srinivasan, *Curr. Sci.* **2006**, *90*, 756 – 757.
[4] D. Lu, T. Takata, N. Saito, Y. Inoue, K. Domen, *Nature* **2006**, *440*, 295 – 297.
[5] O. Coskuner, E. A. A. Jarvis, T. C. Allison, *Angew. Chem.* **2007**, *119*, 7999 – 8001; *Angew. Chem. Int. Ed.* **2007**, *46*, 7853 – 7855.
[6] Y. Tamaura, R. Uehara, N. Hasegawa, H. Kaneko, H. Aoki, *Solid State Ionics* **2004**, *172*, 121 – 124.
[7] H. Ishihara, N. Hasegawa, H. Aoki, H. Kaneko, A. Suzuki, Y. Tamaura, *Solid State Ionics* **2004**, *172*, 117 – 119.
[8] P. Ritterskamp, A. Kuklya, M.-A. Wüstkamp, K. Kerpen, C. Weidenthaler, M. Demuth, *Angew. Chem.* **2007**, *119*, 7917 – 7921; *Angew. Chem. Int. Ed.* **2007**, *46*, 7770 – 7774.
[9] H. Aoki, H. Kaneko, N. Hasegawa, H. Ishihara, A. Suzuki, Y. Tamaura, *Solid State Ionics* **2004**, *172*, 113 – 116.
[10] X. Wu, K. Onuki, *Tsinghua Sci. Technol.* **2005**, *10*, 270 – 276.
[11] S. Ihara, *Bull. Electrotech. Lab.* **1977**, *41*, 259 – 280.
[12] R. Hartung, H.-H. Möbius, *Chem. Ing. Tech.* **1968**, *40*, 592 – 600.
[13] Y. T. Liu, X. Y. Tan, K. Li, *Catal. Rev. Sci. Eng.* **2006**, *48*, 145 – 198.
[14] J. Pére-Ramirez, B. Vigeland, *Angew. Chem.* **2005**, *117*, 1136 – 1139; *Angew. Chem. Int. Ed.* **2005**, *44*, 1112 – 1116.
[15] Z. P. Shao, W. S. Yang, Y. Cong, H. Dong, J. H. Tong, G. X. Xiong, *J. Membr. Sci.* **2000**, *172*, 177 – 188.
[16] C. Chen, S. J. Feng, S. Ran, D. C. Zhu, W. Liu, H. J. M. Bouwmeester, *Angew. Chem.* **2003**, *115*, 5354 – 5356; *Angew. Chem. Int. Ed.* **2003**, *42*, 5196 – 5198A.
[17] B. Cales, J. F. Baumard, *High Temp. High Pressures* **1982**, *14*, 681.
[18] J. Lede, F. Lapicque, J. Villermaux, B. Cales, A. Ounalli, J. F. Baumard, A. M. Anthony, *Int. J. Hydrogen Energy* **1982**, *7*, 939 – 950.
[19] H. Naito, H. Arashi, *Solid State Ionics* **1995**, *79*, 366 – 370.
[20] Y. Nigara, K. Watanabe, K. Kawamura, J. Mizusaki, M. Ishigame, *J. Electrochem. Soc.* **1997**, *144*, 1050 – 1055.
[21] U. Balachandran, T. H. Lee, S. Wang, S. E. Dorris, *Int. J. Hydrogen Energy* **2004**, *29*, 291 – 296.
[22] U. Balachandran, T. H. Lee, S. E. Dorris, *Int. J. Hydrogen Energy* **2007**, *32*, 451 – 456.
[23] T. Schiestel, M. Kilgus, S. Peter, K. J. Caspary, H. H. Wang, J. Caro, *J. Membr. Sci.* **2005**, *258*, 1 – 4.
[24] H. H. Wang, P. Kölsch, T. Schiestel, C. Tablet, S. Werth, J. Caro, *J. Membr. Sci.* **2006**, *284*, 5 – 8.
[25] H. H. Wang, T. Schiestel, C. Tablet, M. Schroeder, J. Caro, *Solid State Ionics* **2006**, *177*, 2255 – 2259.
[26] H. H. Wang, S. Werth, T. Schiestel, J. Caro, *Angew. Chem.* **2005**, *117*, 7066 – 7069; *Angew. Chem. Int. Ed.* **2005**, *44*, 6906 – 6909.
[27] C. Hamel, A. Seidel-Morgenstern, T. Schiestel, S. Werth, H. H. Wang, C. Tablet, J. Caro, *AIChE J.* **2006**, *52*, 3118 – 3125.
[28] H. H. Wang, C. Tablet, T. Schiestel, S. Werth, J. Caro, *Catal. Commun.* **2006**, *7*, 907 – 912.
[29] J. Caro, K. J. Caspary, C. Hamel, B. Hoting, P. Kölsch, B. Langanke, K. Nassauer, T. Schiestel, A. Schmidt, R. Schomäcker, A. Seidel-Morgenstern, E. Tsotsas, I. Voigt, H. H. Wang, R. Warsitz, S. Werth, A. Wolf, *Ind. Eng. Chem. Res.* **2007**, *46*, 2286 – 2294.
[30] M. Schroeder, *Phys. Chem. Chem. Phys.* **2005**, *7*, 166 – 172.
[31] R. Merkle, J. Maier, H. J. M. Bouwmeester, *Angew. Chem.* **2004**, *116*, 5179 – 5183; *Angew. Chem. Int. Ed.* **2004**, *43*, 5069 – 5073.
[32] R. Dittmeyer, J. Caro in *Handbook of Heterogeneous Catalysis*, *Vol. 4* (Eds.: G. Ertl, H. Knözinger, F. Schüth, J. Weitkamp), Wiley-VCH, Weinheim, **2008**, p. 2221.

